JBC RESEARCH ARTICLE

FK506-binding protein-like and FK506-binding protein 8 regulate dual leucine zipper kinase degradation and neuronal responses to axon injury

Received for publication, September 13, 2021, and in revised form, January 21, 2022 Published, Papers in Press, January 29, 2022,
https://doi.org/10.1016/j.jbc.2022.101647

Bohm Lee[1], Yeonsoo Oh[1], Eunhye Cho[1], Aaron DiAntonio[2,3], Valeria Cavalli[4,5,6], Jung Eun Shin[7,8], Hae Woong Choi[1,*], and Yongcheol Cho[1,*]

From the [1]Department of Life Sciences, Korea University, Seoul, Republic of Korea; [2]Department of Developmental Biology, [3]Needleman Center for Neurometabolism and Axonal Therapeutics, [4]Department of Neuroscience, [5]Center of Regenerative Medicine, and [6]Hope Center for Neurological Disorders, Washington University School of Medicine, St. Louis, Missouri, USA; [7]Department of Molecular Neuroscience, Dong-A University College of Medicine, Busan, Republic of Korea; [8]Department of Translational Biomedical Sciences, Graduate School of Dong-A University, Busan, Republic of Korea

Edited by Paul Fraser

The dual leucine zipper kinase (DLK) is a key regulator of axon regeneration and degeneration in response to neuronal injury; however, regulatory mechanisms of the DLK function *via* its interacting proteins are largely unknown. To better understand the molecular mechanism of DLK function, we performed yeast two-hybrid screening analysis and identified FK506-binding protein-like (FKBPL, also known as WAF-1/CIP1 stabilizing protein 39) as a DLK-binding protein. FKBPL binds to the kinase domain of DLK and inhibits its kinase activity. In addition, FKBPL induces DLK protein degradation through ubiquitin-dependent pathways. We further assessed other members in the FKBP protein family and found that FK506-binding protein 8 (FKBP8) also induced DLK degradation. We identified the lysine 271 residue in the kinase domain as a major site of DLK ubiquitination and SUMO3 conjugation and was thus responsible for regulating FKBP8-mediated proteasomal degradation that was inhibited by the substitution of the lysine 271 to arginine. FKBP8-mediated degradation of DLK is mediated by autophagy pathway because knockdown of *Atg5* inhibited DLK destabilization. We show that *in vivo* overexpression of FKBP8 delayed the progression of axon degeneration and suppressed neuronal death after axotomy in sciatic and optic nerves. Taken together, this study identified FKBPL and FKBP8 as novel DLK-interacting proteins that regulate DLK stability *via* the ubiquitin-proteasome and lysosomal protein degradation pathways.

Research in diverse model organisms has yielded critical insights into the molecular mechanisms of neuronal functions under various stress conditions. However, the mechanisms of axon regeneration and degeneration are not fully understood yet. Identifying the molecular mechanisms of regenerative response in injured neurons is required for developing methods promoting functional recovery in the adult mammalian nervous systems. In addition, understanding the mechanisms of axon degeneration is important for identifying therapeutic targets of neurodegeneration. Therefore, it is essential to identify the key molecules regulating axon regeneration and degeneration.

Dual leucine zipper kinase (DLK), a mitogen-activated protein triple kinase 12, is a key regulator of neuronal signal transduction for axon regeneration and degeneration (1, 2). Dual leucine zipper kinase regulates the c-Jun N-terminal kinase (JNK) signaling pathway in neurons under stress conditions and is essential for injury-induced retrograde signaling that is responsible for differential gene expression (3, 4). In addition, DLK is required for axon degeneration as its depletion impairs the process (5). Therefore, identifying DLK regulators is of major relevance for obtaining a better understanding of axon regeneration and degeneration.

Protein degradation pathways are core signaling axes, regulating neuronal responses to a diverse range of stresses (6, 7). Because DLK is a key regulator of neurodegenerative signal transduction, the posttranslational modification of DLK has been studied to understand the mechanisms determining DLK activity, localization, and protein levels (1, 8–10). For example, phosphorylation and palmitoylation of DLK regulate its function (11–13). In addition, DLK protein stability is modulated by the PHR1 E3 ubiquitin ligase and deubiquitinating enzyme USP9X in a key pathway that determines neuronal fate after injury (8–10, 14). Here, we discovered a molecule that interacts with DLK, regulating neuronal responses for axon degeneration. In the present study, we identified FK506-binding protein-like (FKBPL) and FK506-binding protein 8 (FKBP8; FKBP38) as DLK-binding proteins. FK506-binding proteins (FKBPs) belong to the immunophilin family, a group of receptors for immunosuppressive drugs like FK506, rapamycin, and cyclosporin A. FKBPs have a biological function that can regulate or stabilize the components of multiprotein complexes essential to cell function. FKBPL is a divergent immunophilin with distinct functions in disease states, especially appears to have neuroprotective properties.

* For correspondence: Yongcheol Cho, ycho77@korea.ac.kr; Hae Woong Choi, haewoongchoi@korea.ac.kr.

Furthermore, FKBP8 is known to regulate parkin-independent mitophagy, which involves the removal of mitochondria *via* autophagy and lysosomal degradation (15–18). We found that FKBPL is a member of the FKBP family of immunophilins, a group of conserved proteins binding to immunosuppressive drugs, such as FK506, rapamycin, and cyclosporin A. FKBPL and FKBP8 bind to DLK to regulate its kinase activity and degradation *in vitro* and *in vivo*, thus modulating neuronal responses in mouse sciatic and optic nerves after injury.

Results

FKBPL was identified as a DLK-binding protein

To identify DLK-interacting proteins, we performed yeast two-hybrid screening analysis and found *Fkbpl*, *Tedc2*, and *Tuft1* as potential candidates. By analyzing two independent reporter systems, PBN204 and AH109, the *Fkbpl* gene product was determined as the most stable interactor of DLK (Fig. 1, *A* and *B*). FKBPL is a member of the FKBP family, whose members binds to tacrolimus (FK506), an immunosuppressant molecule, and has prolyl isomerase activity (19). Coimmunoprecipitation assays validated the screening result, as exogenously expressed DLK and FKBPL were coimmunoprecipitated in HEK293T cells (Fig. 1*C*).

To determine the region responsible for their interaction, FKBPL-deletion mutants were subjected to coimmunoprecipitation analysis. Deletion of the N-terminal part including the peptidyl-prolyl isomerase (PPI) domain of FKBPL (Δ1 and Δ2) impaired the interaction between DLK and FKBPL (Fig. 1*D*). In addition, the N-terminal region, which includes the kinase domain of DLK, was shown to mediate the interaction, as partial forms of DLK with its N-terminal region (GFP-DLK1 and GFP-DLK2) were able to bind FKBPL (Fig. 1*E*). These results indicated that the N-terminal regions of both proteins were responsible for their interaction, with the FKBPL PPI domain and the DLK kinase domain entering into a stable association to serve as the interaction interface (Fig. 1*F*). Taken together, yeast two-hybrid screening and coimmunoprecipitation analyses revealed that FKBPL was a binding partner of DLK.

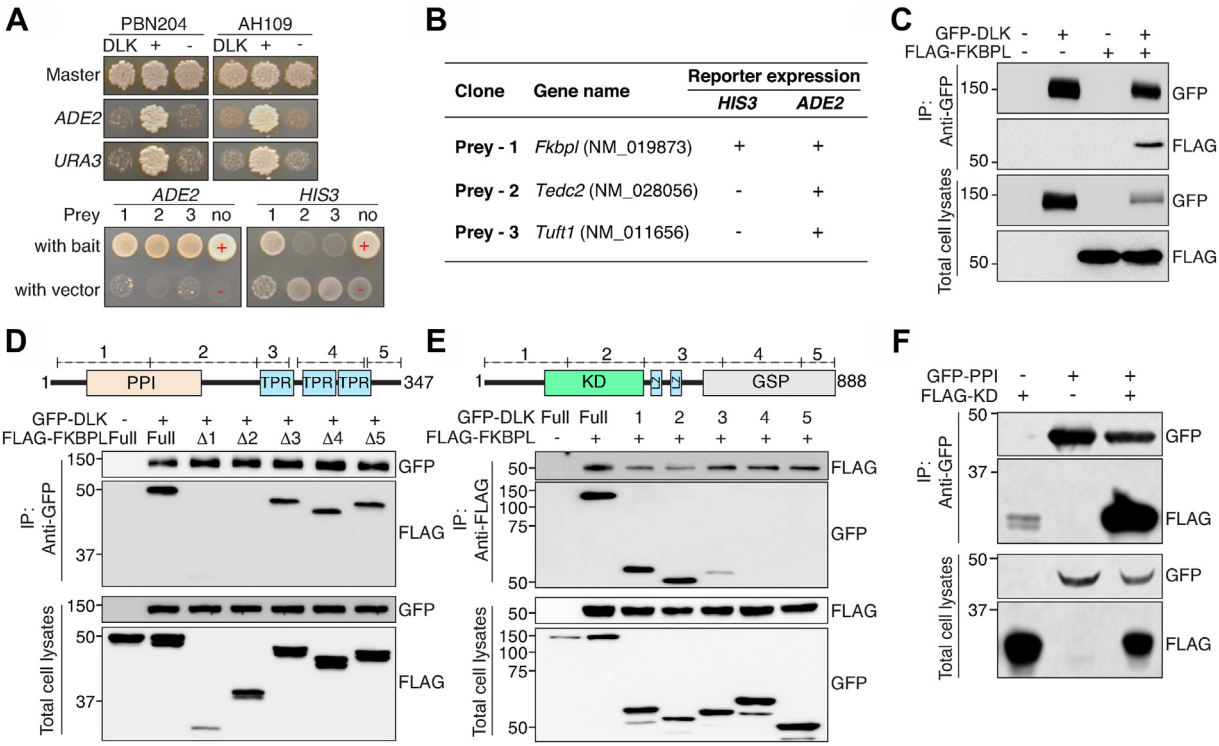

Figure 1. The PPI domain of FKBPL and the kinase domain of DLK are responsible for their interaction. *A*, yeast two-hybrid screening analysis was performed to identify DLK-interacting proteins in yeast strains PBN204 and AH109. Master plates indicate positive controls for the selection. *ADE2* and *URA3* indicate *-Ade* and *-Ura* minimal medium. Dual leucine zipper kinase itself did not activate *ADE2* nor *URA3* gene transcription (*top*). The *ADE2* selection screening identified three preys (1, *Fkbpl*; 2, T*edc2*; and 3, *Tuft1*). *ADE2* minimal medium selection with an additional selection of *HIS3* showed that prey 1 survived and formed the colony. "+" indicates the positive control identical with the *top panel*. *B*, the *Fkbpl* gene product exhibits the most stable association with DLK among the three potential candidates based on two reporter analysis systems. *C*, Western blot analysis of DLK and FKBPL coimmunoprecipitation in HEK293T cells. Green fluorescent protein-DLK and FLAG-FKBPL were cotransfected to HEK293T cells, and the protein lysates were immunoprecipitated using an anti-GFP antibody followed by SDS-PAGE analysis. *D*, schematic diagram of the protein domains of FKBPL and Western blot analysis of DLK co-immunoprecipitation with FKBPL-deletion mutants that were transiently expressed in HEK293T cells. The anti-GFP antibody was used for immunoprecipitation. *E*, schematic diagram of the protein domains of DLK and Western blot analysis for the coimmunoprecipitation of FKBPL with the partial DLK proteins that were transiently expressed in HEK293T cells. An anti-FLAG antibody was used for immunoprecipitation. *F*, Western blot analysis for coimmunoprecipitation of PPI (FKBPL) and KD (DLK). An anti-GFP antibody was used for immunoprecipitation. Green fluorescent protein-PPI and FLAG-KD were expressed in HEK293T cells and subjected to immunoprecipitation analysis under nondenaturation conditions. DLK, dual leucine zipper kinase; GSP, Gly, Ser, and Pro-rich domain; KD, kinase domain; LZ, leucine zipper motif; PPI, peptidyl-prolyl isomerase; SDS-PAGE, sodium dodecyl sulfate-polyacrylamide gel electrophoresis; TPR, tetratricopeptide repeat domain.

FKBPL inhibited DLK kinase activity and induced DLK degradation

As FKBPL bound to DLK's kinase domain, we performed *in vitro* kinase assays to investigate whether DLK kinase activity was modulated *via* its association with FKBPL (1) (Fig. 2*A*). Green fluorescent protein-DLK was expressed with or without FLAG-FKBPL coexpression in HEK293T cells, immunopurified using the anti-GFP antibody, and incubated with the substrate glutathione-S-transferase (GST)-mitogen-activated protein kinase kinase 4 (MKK4) *in vitro* (Fig. 2, *A* and *B*). Western blot analysis indicated that GST-MKK4 was phosphorylated after incubation with GFP-DLK, as previously reported (1). However, MKK4 phosphorylation was significantly reduced when incubated with the FLAG-FKBPL-associated DLK immunoprecipitant, indicating that the association of FKBPL inhibited DLK kinase activity (Fig. 2, *B* and *C*). As FKBPL was bound to the kinase domain, this association might physically hinder substrates from interacting with the DLK kinase domain.

Dual leucine zipper kinase activity was required for its stabilization, and the kinase activity-dead mutations caused destabilization of DLK at the protein level (8). As FKBPL bound to DLK and inhibited its kinase activity, we tested the protein level of DLK with FKBPL coexpression and found that DLK protein levels were significantly lower when FKBPL was coexpressed in HEK293T cells (Fig. 2, *D* and *E*). However, FKBPL-mediated DLK suppression was not prevented by applying a broad-spectrum inhibitor of serine proteases, cysteine proteases, metalloproteases, and calpains (Fig. 2*D*). In addition, caspase inhibitor treatment had no effect on DLK reduction (Fig. 2*E*). Therefore, the direct cleavage by proteases might not be responsible for the FKBPL-induced reduction of DLK protein levels. These results indicated that FKBPL inhibits DLK kinase activity and reduces its protein stability.

FKBPL and FKBP8 induced the lysosomal degradation of DLK

As FKBPs are a group of proteins containing an FK506-binding domain and a PPI domain (20–24), we tested other FKBP proteins to monitor the reduction of DLK protein levels. First, we reviewed the expression levels of *Fkbp* mRNA in mouse L4,5 dorsal root ganglion (DRG) tissues and sciatic nerves from our previously published datasets (3, 25, 26). In addition, the microarray dataset from cultured mouse embryonic DRG neurons was presented as circles with size based on the relative levels of neuronal expression (Fig. 3*A*) (27). *Fkbp*3, *Fkbp*4, *Fkbp*8, and *Fkbp*12 transcripts were more abundantly expressed than the rest in adult mouse DRGs and sciatic nerves (Fig. 3*A*). In addition, the neuronal expression profiles of *Fkbp* mRNAs indicated that *Fkbp*4, *Fkbp*8, and *Fkbp*12 were relatively upregulated compared to other family members, which was observed in embryonic DRG neurons cultured without non-neuronal cells (27). This analysis implied that FKBP4, FKBP8, and FKBP12 were potential DLK-regulating FKBPs in sensory neurons. Next, we tested DLK destabilization under coexpression of the FKBPs. FKBPL coexpression in HEK293T cells decreased DLK protein levels down to 32% compared to control levels (Fig. 3*B*). Western blot analysis indicated that FKBP8 most potently lowered DLK protein levels, similarly to FKBPL, whereas FKBP3 and FKBP4 had a mild effect on DLK protein levels (Fig. 3, *B* and *D*). In addition, coimmunoprecipitation analysis indicated that both human and mouse FKBP8 were associated with DLK, whereas FKBP4 did not interact with it (Fig. 3*C*).

FKBP8 regulates parkin-independent mitophagy, which facilitates the removal of mitochondria *via* autophagy and lysosomal degradation (15–18, 22). As FKBP8 bound to DLK and lowered its protein levels, we tested whether FKBP8- or FKBPL-induced DLK suppression was mediated *via* lysosomal degradation. When HEK293T cells were incubated with

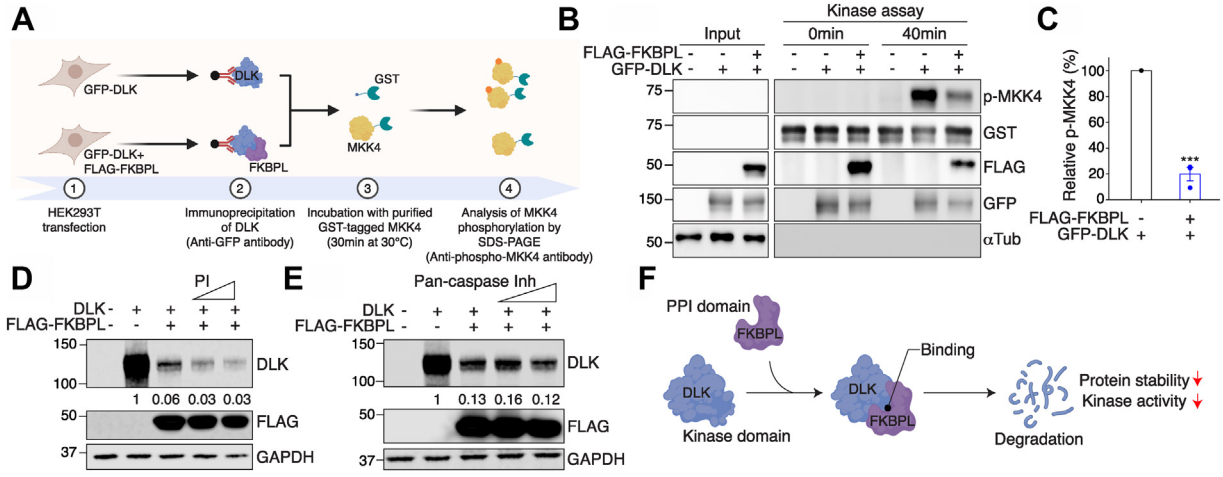

Figure 2. FKBPL inhibited the kinase activity of DLK and reduced DLK protein levels. *A*, schematic of the DLK *in vitro* kinase assay. Green fluorescent protein-DLK was expressed in HEK293T cells with or without FLAG-FKBPL coexpression. Immunopurified GFP-DLK was incubated in reaction buffer containing the GST-MKK4 substrate that was transiently expressed in HEK293T cells and purified independently. *B*, Western blot analysis for the *in vitro* kinase assays. Phosphorylated MKK4 was detected using anti-phospho-MKK4 antibody. Anti-GST, -FLAG, and -GFP antibodies were used for detecting GST-MKK4, FLAG-FKBPL, and GFP-DLK protein, respectively, from input and kinase reaction samples. An anti-α-tubulin antibody was used as the loading control. *C*, quantification of relative p-MKK4 levels from (*B*) (n = 3 for each condition; ***$p < 0.001$ by *t* test; mean ± S.E.M.). *D* and *E*, Western blot analysis for GFP-DLK and FLAG-FKBPL protein levels under protease inhibitor (PI) (*D*) or pan-caspase inhibitor (Pan-caspase Inh) (*E*) treatment at different doses. Dual leucine zipper kinase and FLAG-epitope-tagged FKBPL were expressed in HEK293T cells. *F*, schematic model of the interaction between DLK and FKBPL. DLK, dual leucine zipper kinase; MKK4, mitogen-activated protein kinase kinase 4.

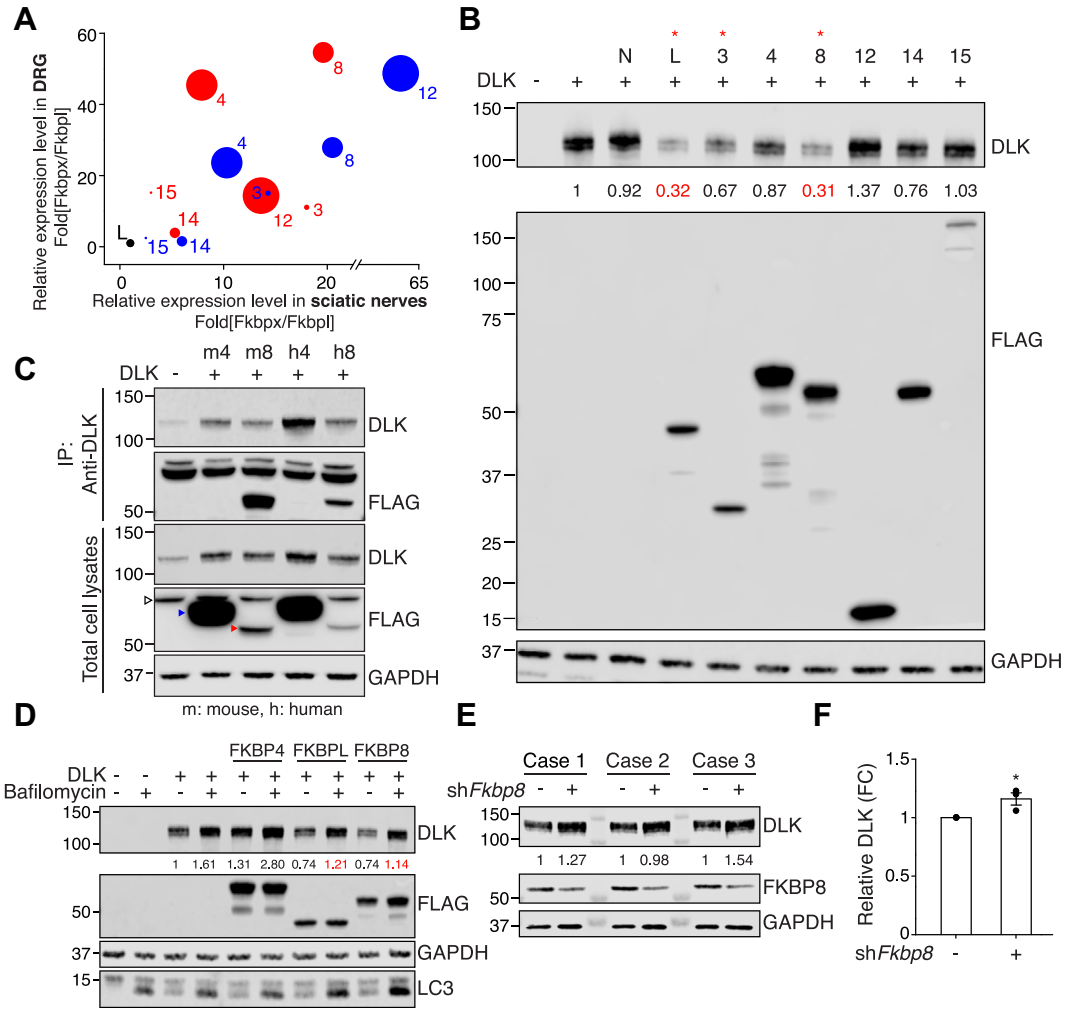

Figure 3. FKBPL and FKBP8 induced lysosome-dependent DLK degradation. *A*, comparative analysis of relative expression levels in mouse L4,5 dorsal root ganglion (DRG) tissues, sciatic nerve tissues, and cultured embryonic DRG neurons (3, 25–27). *Red* and *blue circles* indicate *Illumina* short-read sequencing and *Oxford Nanopore direct RNA* long-read sequencing, respectively. *Circle sizes* indicate relative levels of microarray data from cultured embryonic DRG neurons. *B*, Western blot analysis for the expression of DLK with FKBPs (N; null vector, L; FKBPL, 3; FKBP3, 4; FKBP4, 8; FKBP8, 12; FKBP12, 14; FKBP14, 15; FKBP15). The number indicates normalized relative intensity. Dual leucine zipper kinase and FLAG-epitope-tagged FKBP protein family members were expressed in HEK293T cells and subjected to SDS-PAGE. *C*, Western blot analysis for the immunoprecipitation of DLK with mouse (m) and human (h) FKBP4/8 that was overexpressed in HEK293T cells. *Empty arrowhead*, non-specific band; *blue arrowhead*, FKBP4; *red arrowhead*, FKBP8. *D*, Western blot analysis for the expression of DLK and FKBPL/4/8 expressed in HEK293T cells with or without bafilomycin A1 treatment. The numbers indicate the normalized relative intensity. *E*, Western blot analysis of DLK protein levels under *Fkbp8* knockdown (sh*Fkbp8*) by lentiviral delivery in primary cultured embryonic DRG neurons. The numbers indicate the normalized relative intensity. *F*, statistical analysis of (*E*) (FC, fold change; n = 3 for each condition; $^*p < 0.05$ by *t* test; mean ± S.E.M.). DLK, dual leucine zipper kinase.

bafilomycin A1, FKBPL- and FKBP8-induced DLK degradation was inhibited, suggesting that DLK was degraded *via* the lysosome (Fig. 3*D*). Moreover, the basal protein levels of DLK without FKBP8 or FKBPL coexpression were upregulated under bafilomycin A1 treatment, further suggesting lysosomal degradation as a potential pathway mediating DLK protein suppression (Fig. 3*D*). To validate the result in neurons, endogenous FKBP8 was knocked down by introducing shRNA-containing lentivirus into cultured embryonic DRG neurons. Endogenous DLK proteins from primary cultured embryonic DRG neurons were increased by knocking down *Fkbp8*, indicating that FKBP8 regulated DLK protein stability in these cells (Fig. 3, *E* and *F*). Taken together, we demonstrated that FKBPL and FKBP8 are DLK-interacting proteins that induce its degradation *via* the lysosome.

The kinase domain of DLK was a major target for its ubiquitination and SUMOylation

Dual leucine zipper kinase protein degradation is regulated by the PHR1 E3 ligase (6, 7). As FKBPL- or FKBP8-induced DLK protein downregulation required bafilomycin-sensitive lysosomal function, we tested whether FKBP8-dependent DLK protein reduction was mediated *via* ubiquitin-dependent degradation. First, DLK was subjected to ubiquitination assays by transiently expressing HA epitope-tagged ubiquitin in HEK293T cells. Denaturation immunoprecipitation indicated that HA-ubiquitin was covalently conjugated with DLK in HEK293T cells (Fig. 4*A*, dimethyl sulfoxide). When FKBP8 was coexpressed with DLK in HEK293T cells, ubiquitinated DLK proteins were significantly reduced, which was reversed by incubating transfected HEK293T cells with

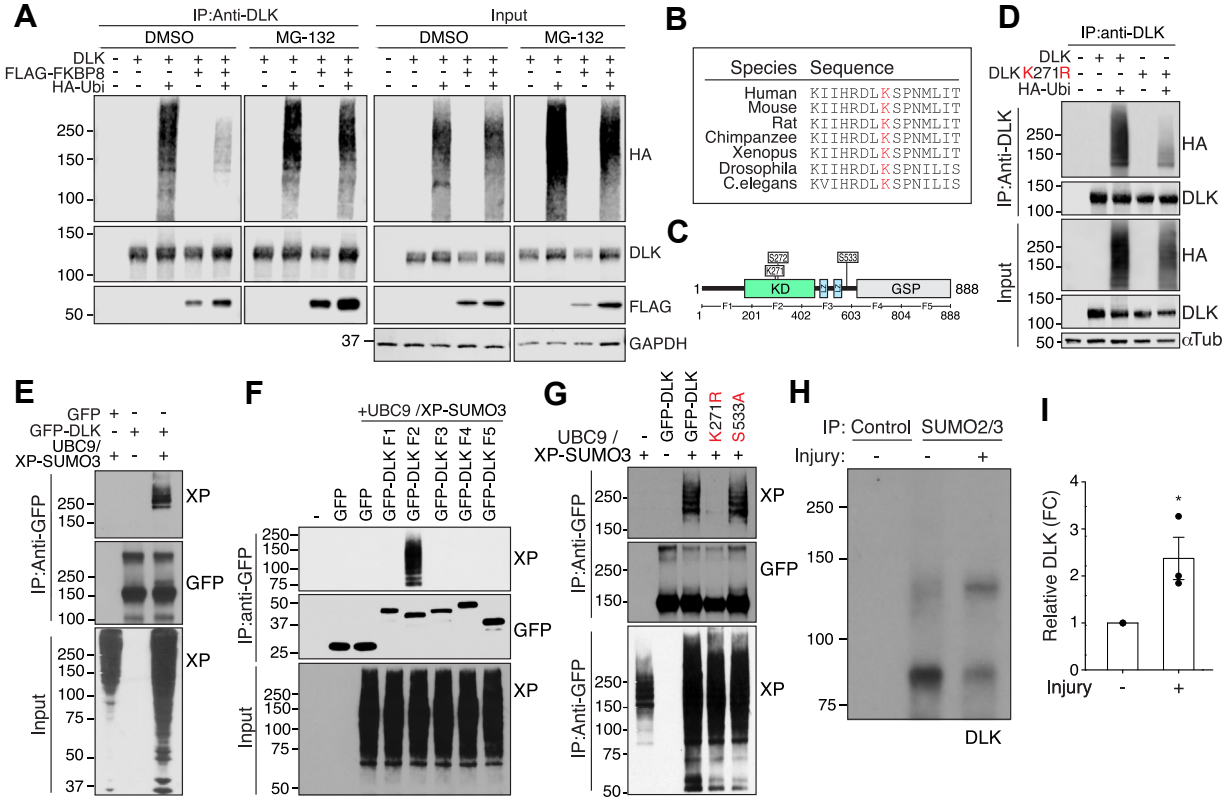

Figure 4. The K271 residue within the kinase domain is a major target of DLK ubiquitination and SUMOylation. *A*, Western blot analysis for the immunoprecipitation assays of DLK, FLAG-FKBP8, and HA-ubiquitin (HA-Ubi) with or without MG-132 treatment. Dual leucine zipper kinase, FLAG-FKBP8, and HA-ubiquitin were expressed from HEK293T cells and immunoprecipitated using an anti-DLK antibody under denaturing condition, as described in Experimental procedures. HEK293T cells were incubated in culture medium with or without 10 μM MG-132 for 6 h. *B*, alignment of amino acid sequences adjacent to the lysine at 271 in the kinase domain of DLK in various species (*Red*; lysine at 271). *C*, schematic diagram of DLK protein domains. Three serine residues subjected to JNK phosphorylation were indicated. *D*, Western blot analysis for denaturing immunoprecipitation assay with WT DLK and the DLK K271R mutant with HA-ubiquitin expression (HA-Ubi). *E*, Western blot analysis for SUMO-denaturation immunoprecipitation assays with GFP-DLK, UBC9, and XP-SUMO3 (XP, Xpress epitope). *F*, Western blot analysis for SUMO-denaturation immunoprecipitation with the partial DLK proteins, as indicated in Figure 1*E*. *G*, Western blot analysis for SUMO-denaturation immunoprecipitation assays with WT DLK, DLK K271R mutant, and DLK S533A mutant. The *in vitro* ubiquitination and SUMOylation assays in (*D–G*) were done with cultured HEK293T cells. Transiently expressed DLK was immunoprecipitated under denaturation condition as described in Experimental procedures. *H*, Western blot analysis of SUMO-denaturation immunoprecipitation assays from the tissue lysates of sciatic nerves with or without injury. Sciatic nerves were dissected at 24 h after axotomy, and the lysates were immunoprecipitated using anti-SUMO2/3 antibody under boiling denaturation conditions. *I*, statistical analysis of (*H*) (FC, fold change; n = 3 for each condition; $*p < 0.05$ by *t* test; mean ± S.E.M.). DLK, dual leucine zipper kinase; GSP, Gly, Ser, and Pro-rich domain; JNK, c-Jun N-terminal kinase; KD, kinase domain; LZ, leucine zipper motif; SUMO, small ubiquitin-like modifier.

MG-132, an inhibitor of ubiquitin-dependent protein degradation (Fig. 4*A*, MG-132). These data indicated that FKBP8 induced DLK degradation *via* the ubiquitin-dependent protein degradation pathway.

To identify lysine residues responsible for ubiquitination, we assessed lysine residues within the kinase domain of DLK as the site of FKBPL interaction. We noted that K271 was followed by S272, a serine residue known to be phosphorylated by JNK and essential for DLK kinase activity, as the DLK^{S272A} mutant had none (8). The serine residue at 272 was among the top three sites for JNK-dependent DLK phosphorylation and the only serine residue among these residues (Fig. 4*C*). Moreover, this region was highly conserved across species (Fig. 4*B*). Therefore, we hypothesized that it acts as an interface for DLK regulation by modulating its kinase activity and/or its stability, with K271 undergoing posttranslational modifications, including ubiquitination.

To explore this, ubiquitination experiments on the DLK^{K271R} mutant revealed that replacing this lysine with arginine (DLK^{K271R} mutant) dramatically lowered the efficacy of ubiquitin conjugation to DLK in HEK293T cells (Fig. 4*D*). This indicated that the lysine at 271 was indeed a major target site of DLK ubiquitination. Furthermore, K271 also served as the site of SUMOylation (small ubiquitin-like modifier) as DLK was conjugated with SUMO3 when SUMO3/Ubc9 was coexpressed in HEK293T cells, whereas the K271R mutant was not (Fig. 4, *E–G*). To assess DLK SUMOylation *in vivo*, mouse sciatic nerves were axotomized and dissected at 24 h after injury. The nerves were lysed in denaturing conditions and subjected to SUMO2/3 immunopurification. Western blot analysis indicated that SUMOylated DLK protein levels were increased when the nerves were injured (Fig. 4, *H* and *I*). Taken together, these results revealed that K271 was the major site of ubiquitination and SUMO3 conjugation.

FKBP8-mediated ubiquitin-dependent DLK degradation

As the K271 residue was responsible for DLK ubiquitination, we investigated whether this site was required for FKBP8-induced DLK degradation. Western blot analysis indicated that the DLK^{K271R} mutant was resistant to FKBP8-induced

degradation (Fig. 5*A*). Introducing a substitution mutation at K271 inhibited FKBP8-mediated DLK degradation (Fig. 5*B*). This result indicated that the ubiquitination of DLK was required for its FKBP8-mediated degradation, suggesting that ubiquitinated DLK protein might be recruited to the FKBP8-associated protein degradation complex. In addition, the DLK^{K271R} mutant exhibited a less efficient association with FKBP8, implying that DLK ubiquitination at K271 might modulate interaction efficiency between DLK and FKBP8 (Fig. 5*C*).

To validate the result in neurons, endogenous DLK protein levels were monitored by Western blot analysis of primary cultured embryonic DRG neurons with or without FLAG-FKBP8 overexpression (Fig. 5*D*). Endogenous DLK protein was significantly reduced when FKBP8 was overexpressed in cultured DRG neurons. However, the MG-132 application protected DLK against degradation in FKBP8-overexpressing DRG neurons. These data indicated that FKBP8 induced DLK degradation *via* the MG-132-sensitive pathway in DRG

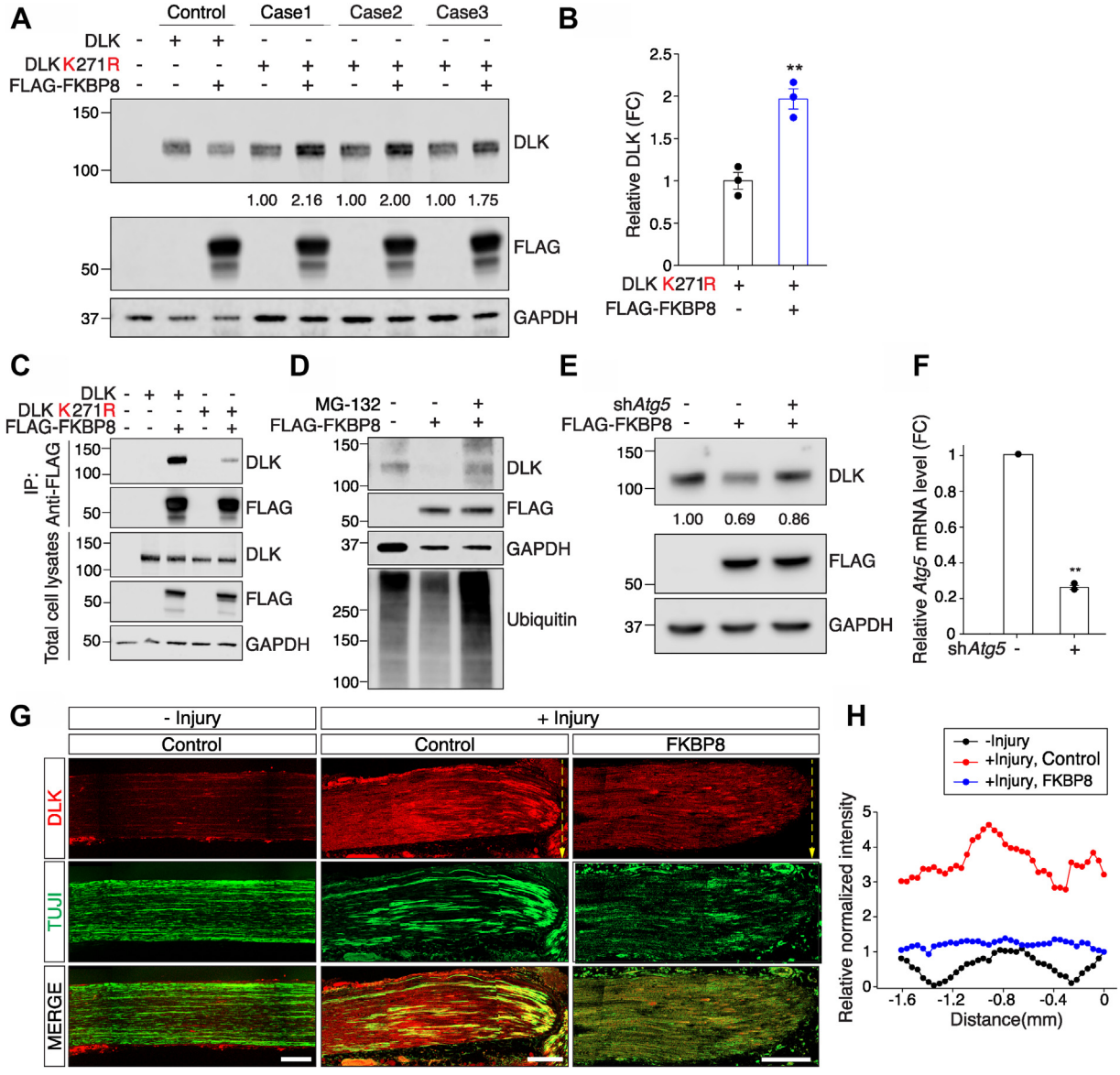

Figure 5. FKBP8 mediates ubiquitin-dependent DLK degradation. *A*, Western blot analysis for the expression of DLK, its K271R mutant, and FKBP8 in HEK293T cells. The numbers indicate the normalized relative intensity. *B*, statistical analysis of (A) (n = 3 for each condition; $^{**}p < 0.01$ by *t* test; mean ± S.E.M.). *C*, Western blot analysis for the immunoprecipitation assays of FKBP8 with DLK and the K271R mutant. Dual leucine zipper kinase, DLK K271R, and FLAG-epitope-tagged FKBP8 were expressed in HEK293T cells. The protein lysates were immunoprecipitated using an anti-FLAG antibody followed by SDS-PAGE analysis. *D*, Western blot analysis for validating DLK levels by the expression of FKBP8 with or without MG-132 treatment in primary cultured embryonic DRG neurons. Embryonic DRG neurons were incubated with or without 10 μM MG-132 treatment for 6 h and lysed for Western blot analysis. *E*, primary cultured embryonic DRG neurons were infected by lentivirus of FLAG-FKBP8 with or without *Atg5*-shRNA at DIV2 and lysed for Western blot analysis. *F*, relative expression of *Atg5* mRNA analyzed *via* RT-qPCR (FC, fold change; n = 3; mean ± SEM; $^{**}p < 0.01$ by *t* test). *G*, sciatic nerves from AAV-control- or AAV-FKBP8-injected mice were ligated and dissected at 24 h after injury. Longitudinal sections were immunostained with the anti-DLK antibody and TUJI antibody. *Yellow dotted arrows* indicate the injury site. The scale bar represents 200 μm. *H*, relative normalized intensity of DLK was plotted with x-axis of distance and y-axis of relative ratio. AAV, adeno-associated virus; DLK, dual leucine zipper kinase; DRG, dorsal root ganglion; SDS-PAGE, sodium dodecyl sulfate-polyacrylamide gel electrophoresis.

neurons. In addition, FKBP8-induced DLK degradation was retarded when *Atg5* was knocked down in cultured primary DRG neurons (Fig. 5, *E* and *F*), suggesting that autophagy was involved in FKBP8-mediated DLK degradation. To test this notion *in vivo*, mice were injected with adeno-associated virus (AAV) AAV-FKBP8, as described in Experimental procedures, and subjected to sciatic nerve ligation injury (Fig. 5*G*). Immunohistochemical analysis revealed that uninjured sciatic nerves had low amounts of DLK protein. When sciatic nerves were ligated for introducing injury, DLK protein was accumulated at the injury site (+Injury in Fig. 5, *G* and *H*). However, DLK accumulation was reduced under FKBP8 overexpression. These results showed that FKBP8 regulated neuronal DLK protein levels *via* ubiquitin and autophagy pathways.

In vivo *gene delivery of* Fkbp8 *delayed axon degeneration in mouse sciatic nerves and enhanced the viability of retinal ganglion cell neurons after optic nerve injury*

As FKBP8 interacted with DLK to regulate its degradation, we monitored neuronal injury responses under FKBP8 overexpression *in vivo*. *In vivo* gene delivery using an AAV successfully established FKBP8 overexpression in DRG tissues (Fig. 6, *A*–*C*). To test axon degeneration *in vivo*, sciatic nerves from AAV-control- or AAV-FKBP8-injected mice were cut, and the distal part that was physically disconnected from the cell body was dissected 3 days after axotomy (Fig. 6*A*). Immunohistological analysis revealed that FKBP8 overexpression delayed axon degeneration in sciatic nerves because cross-sectioned sciatic nerves of the distal nerve segments exhibited more TUJ1-positive axons in FKBP8-overexpressing mice (Fig. 6, *D* and *E*). By assessing the number of axonal cross-sections with TUJ1-positive immunostaining within the unit area, we observed that control sciatic nerves had an average of 11.8 ± 2.4 intact axons with a diameter of more than 5 μm, whereas sciatic nerves from FKBP8-overexpressing mice had an average of 20.0 ± 3.2 axons per unit area, a nearly two-fold increase.

As DLK is responsible for retinal ganglion cell (RGC) apoptosis after optic nerve crush (ONC) injury (8, 10), we tested whether FKBP8 overexpression prevented RGC death after ONC. Sections of mouse retina were prepared 3 days after ONC injury and immunostained for BRN3A as a marker of RGCs (Fig. 6*F*). We observed a significant reduction in BRN3A-positive RGCs in the retina with ONC injury compared to control mice (Fig. 6*G*). Control mice had an average of 13.2 ± 1.0 BRN3A-positive cells, whereas ONC injury reduced the number to 6.2 ± 0.6 per unit area. However, the FKBP8-overexpressing mice had an average of 12.4 ± 0.8 BRN3A-positive cells 3 days after optic nerve injury (Fig. 6*H*). These results indicated that injury-induced death-signaling after ONC was down-regulated under FKBP8 overexpression, altogether suggesting that FKBP8 is a potential target in the molecular mechanism regulating injury-related axon degeneration and neuronal death.

Discussion

DLK is a core protein responsible for the regulation of neuronal responses to injury. As DLK plays a role in both axon regeneration and degeneration, it has been referred to as a "double-edged sword" in damaged neural tissue (28). Therefore, it is essential to determine the molecular mechanisms regulating DLK function to obtain a better understanding of neuronal responses to stress. In this study, we identified DLK-interacting proteins FKBPL and FKBP8 as the regulators of DLK degradation and kinase activity. FKBPL and FKBP8 bound to the kinase domain of DLK to inhibit its activity. In addition, FKBP8 induced the degradation of ubiquitinated DLK through the lysosomal degradation pathway. *In vivo* gene delivery of FKBP8 delayed axon degeneration in sciatic nerves after axotomy and exhibited a protective effect against RGC death after ONC injury.

Dual leucine zipper kinase protein levels are differentially regulated when neurons are subjected to specific stressors such as axotomy and microtubule-stabilizing/destabilizing agents (29–34). Moreover, elevated DLK protein levels result in neuronal death in optic nerve injury models (8, 10). Therefore, identifying the molecular mechanism underlying DLK protein turnover is important for understanding how neuronal fate is determined in response to injury. PHR1 E3 ligase and the deubiquitinating enzyme USP9X are the key regulators of DLK protein levels (8, 14). Herein, we expand the knowledge on DLK protein degradation through the identification of lysine 271 as the residue responsible for the DLK ubiquitination and SUMOylation at the kinase domain, suggesting that competition between ubiquitination and SUMOylation may occur at this residue. In addition, the lysine at 271 is required for ubiquitin-dependent DLK lysosomal degradation. In conclusion, the FKBPL- and FKBP8-mediated DLK protein degradation *via* the lysosome represents a new direction for the manipulation of DLK protein levels *in vivo* for the study of neuropathological and neurodegenerative conditions.

Experimental procedures

Mice and surgical procedures

CD-1:Crl:CD-1(ICR) and C57BL/6J mice were used in the present study. All animal husbandry and surgical procedures were approved by the Korea University Institutional Animal Care & Use Committee (KU-IACUC). Surgery was performed under isoflurane anesthesia following regulatory protocols. Sciatic nerve injury experiments were performed as previously described (35). Briefly, anesthetized animals were subjected to unilateral exposure of the sciatic nerve at thigh level, and a crush injury was inflicted with fine forceps for 10 s (36).

Lentiviral constructs and AAV-mediated in vivo *gene delivery*

Lentivirus-mediated gene delivery was used to knockdown target mRNA in embryonic DRG neurons. Lentivirus was produced with Lenti-X packaging Single Shots (Takara, 631275), as previously described (37). For *in vitro* gene

delivery, lentivirus was applied to embryonic DRG neuron cultures at DIV2. To knock down *Fkbp8* or *Atg5 in vitro*, shRNA targeting sequences identified by the BROAD Institute (TRCN0000280135 or TRCN0000375754) were synthesized (Bionics) and ligated into a pLKO.1 lentiviral vector with *AgeI*/*EcoRI* restriction sites. Lentivirus was produced using Lenti-XTM Packaging Single Shot (Qiagen, 631276), concentrated with a Lenti-XTM Concentrator (Qiagen, 631232), and quantified using a Lenti-XTM GoStixTM Plus kit (Qiagen, 631280), as previously described (38). Knockdown efficiency was confirmed using RT-qPCR. To deliver genes *in vivo*, 10 μl of AAV (serotype 9) encoding GFP- and FLAG-tagged mouse *Fkbp8* was injected into neonatal CD-1 mice (postnatal day 1) *via* facial vein injection using a Hamilton syringe (Hamilton, 1710 syringe with a 33G/0.75-inch small hub removable needle). The expression of GFP and the target gene in sciatic nerves and DRGs was confirmed *via* immunoblot, immunohistochemistry, and RT-qPCR analysis.

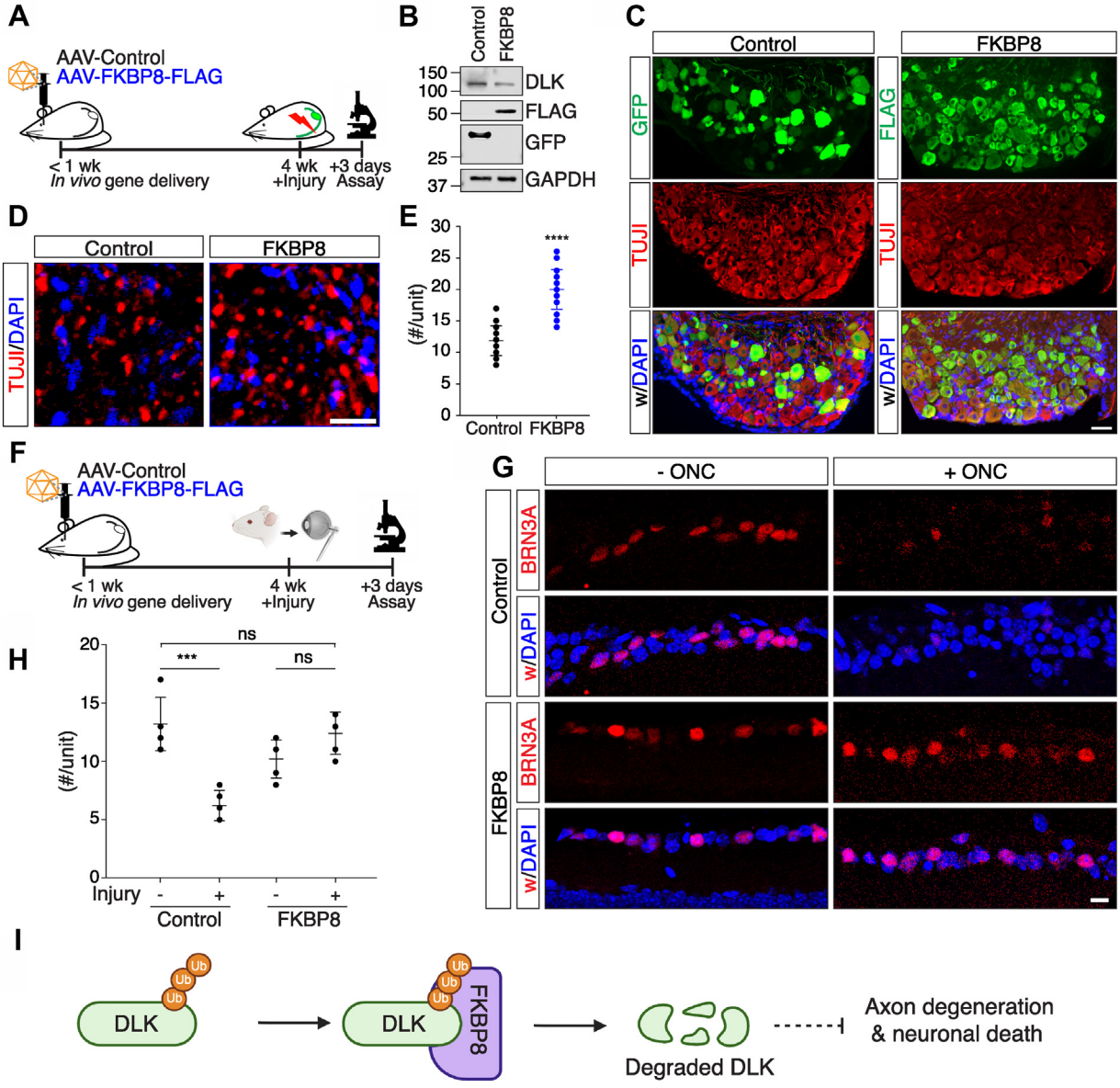

Figure 6. *In vivo* gene delivery of FKBP8 delayed axon degeneration and enhanced the viability of RGC neurons. *A*, experimental scheme of gene delivery for *in vivo* axon regeneration and degeneration assays using mouse sciatic nerves (wk, week). *B*, Western blot analysis of DLK, GFP, and FLAG-FKBP8 proteins in L4,5 DRG tissue lysates from AAV-injected mice. *C*, immunohistochemistry of mouse L4,5 DRG sections from AAV-injected mice, stained with anti-GFP for GFP-injected mice (Control), and anti-FLAG for FLAG-FKBP8-injected mice. The scale bar represents 50 μm. *D*, *in vivo* degeneration assays for sciatic nerves. Representative cross-sections of the sciatic nerves from control or FKBP8-expressing mice. The scale bar represents 25 μm. *E*, statistical analysis for (*D*) (n = 3 for each condition; $^{****}p < 0.0001$ *via t* test; mean ± S.E.M.). *F*, experimental scheme for *in vivo* gene delivery to mouse retinas (wk; week). *G*, representative longitudinal sections of the retinas from control or FKBP8-expressing mice. The scale bar represents 10 μm. *H*, quantification of the number of BRN3A-stained RGCs with or without injury (n = 5 for each condition; $^{***}p < 0.001$; ns, not significant *via t* test; mean ± S.E.M.). *I*, schematic illustration of FKBP8-mediated DLK degradation. AAV, adeno-associated virus; DLK, dual leucine zipper kinase; DRG, dorsal root ganglion; RGC, retinal ganglion cell.

Antibodies and chemicals

The following antibodies were used: anti-GFP (Santa Cruz, sc-9996 for coimmunoprecipitation; Abcam, ab32146 for immunoblots), anti-FLAG horseradish peroxidase-conjugated (Sigma, A8592), anti-p-SEK1/MKK4 (Cell Signaling, CST-9151), anti-GST (Santa Cruz, sc-138), anti-alpha-tubulin (Santa Cruz, sc-53030), anti-DLK (ThermoFisher Scientific, PA5-32173 for coimmunoprecipitation and immunohistochemistry; Antibodies Incorporated, 75-355 for immunoblot), anti-GAPDH (Santa Cruz, sc-32233), anti-LC3A/B (Cell Signaling, CST-12741), anti-HA (Abcam, ab9110), anti-Xpress (ThermoFisher Scientific, R910-25), anti-SUMO2/3 (Abcam, ab3742), anti-FLAG (Cell Signaling, 14793S), anti-BRN3A Alexa Fluor 594 (Santa Cruz, sc-8429 AF594), and anti-beta III tubulin (Abcam, ab41489). We dissolved all chemicals in dimethyl sulfoxide (Sigma, D8418-250ML) except for vincristine (Sigma, V8879), which was dissolved in methanol. Controls were treated with dimethyl sulfoxide as vehicle or methanol in the case of vincristine controls. We used vincristine at 200 nM, bafilomycin (Sigma, B1793) at 100 nM, caspase inhibitor (Sigma, 400012) at 1 and 5 μM, pan-caspase inhibitor (R&D systems, FMK001) at 10 and 50 μM, and MG-132 (Sigma, M7449) at 10 μM.

Plasmids

An expression plasmid for full-length Myc-DDK-tagged Mouse *Fkbp3* (MR202616), *Fkbp4* (MR227193), *Fkbp8* (MR220865), *Fkbp12* (MR200405), *Fkbp14* (MR202290), and *Fkbp15* (MR220579) were purchased from Origene. An expression plasmid for full-length Myc-DDK-tagged Human *FKBP4* (RC200713) and *Fkbp8* (RC216639) were purchased from Origene. The constructs were transfected into HEK293T cells using Lipofectamine 2000 (Thermo, 11668-019).

Yeast two-hybrid screening

Yeast two-hybrid analysis was performed using a contract with Panbionet (http://panbionet.com/). The bait was generated from the mouse *Map3k12* CDS (DLK, NM_001163643, full length, 887 amino acids, 2667) and cloned into the *Xmal*/*SalI* sites of a pGBKT7 vector with the primers 5′-CGC CCG GGG GCC TGC CTC CAT GAA ACC C-3′ and 5′- GG CTC GAG TCA TGG AGG AAG GGA GGC T-3′. Various DLK baits were used to screen multiple complementary DNA libraries derived from mouse embryos.

Western blot analysis and coimmunoprecipitation assays

To study protein–protein interactions, plasmids containing mouse *Map3k12* and mouse FLAG-tagged *Fkbpl*/*Fkbp8* were transfected into HEK293T cells using Lipofectamine 2000 (Thermo, 11668-019) following the manufacturer's instructions. Cell lysates were prepared in 1× SDS buffer (63 mM Tris pH 6.8, 2% SDS, and 10% glycerol) and then boiled for 10 min at 95 °C. After centrifugation, protein concentration in the supernatant was determined *via* DC protein assays (Biorad, 5000116) with bovine serum albumin solutions as standards. Equal amounts of protein were loaded into 1× Mops running buffer for sodium dodecyl sulfate-polyacrylamide gel electrophoresis (SDS-PAGE) and transferred onto a nitrocellulose membrane. The membranes were blocked with 5% skim milk dissolved in 1× TBS with 0.1% Tween-20 (TBS-T) for 1 h, incubated with primary antibodies overnight at 4 °C, and washed three times with TBS-T. The blots were then incubated with secondary antibodies for 1 h and washed three times with TBS-T. Protein expression levels were analyzed *via* enhanced chemiluminescence using Odyssey (Li-Cor). Green fluorescent protein-tagged *Map3k12-* and FLAG-tagged *Fkbpl*-transfected HEK293T cells were lysed in immunoprecipitation (IP) buffer (0.5% NP40, 150 mM NaCl, 20 mM Tris–HCl pH 7.5) containing a protease inhibitor cocktail (Roche). Green fluorescent protein-DLK was immunoprecipitated with an anti-GFP antibody prebound to Dynabeads Protein A (Thermo, 10001D) from input lysates for 16 h at 4 °C. The precipitates were washed four times using DynaMag-2 (Thermo, 12321D) and subjected to SDS-PAGE for Western blot analysis. *Map3k12-* and FLAG-tagged mouse *Fkbp4*/*Fkbp8-* or FLAG-tagged human *FKBP4*/*FKBP8*-transfected HEK293T cells were lysed in IP buffer (0.5% NP40, 150 mM NaCl, 20 mM Tris–HCl pH 7.5) containing a protease inhibitor cocktail (Roche). Dual leucine zipper kinase was immunoprecipitated with an anti-DLK antibody prebound to Dynabeads Protein A (Thermo, 10001D) from input lysates for 16 h at 4 °C.

For SUMO-denaturation immunoprecipitation assays, GFP-tagged *Map3k12*, *Ubc9*, and Xp-tagged *SUMO3*-transfected HEK293T cells were lysed in denaturation IP buffer (5% SDS, 30% glycerol, 0.15 M Tris–HCl pH 6.7) and then boiled for 10 min at 95 °C. After vortexing, IP buffer (0.5% NP40, 150 mM NaCl, 20 mM Tris–HCl pH 7.5), containing a protease inhibitor cocktail (Roche), was added with anti-GFP antibody prebound to Dynabeads Protein A (Thermo, 10001D).

RNA extraction and RT-qPCR

RNA extraction from cultured embryonic DRG neurons at DIV5 was performed using the RNAqueous Total RNA isolation kit (Thermo Fisher Scientific, AM1931) as per manufacturer's instructions. The RevertAid Reverse Transcriptase (Thermo Fisher Scientific, EP0441) was used for complementary DNA synthesis and the PowerUP SYBP green master mix (Thermo Fisher Scientific, A25918) for PCR. Relative expression levels were determined *via* the cycle threshold method, with *Gapdh* used as an internal control.

In vitro *kinase assays*

Dual leucine zipper kinase activity was assessed as previously described (1). HEK293T cells were transfected with GFP-tagged *Map3k12* or FLAG-tagged *Fkbpl* individually using Lipofectamine 2000 (Thermo, 11668-019). Cell lysates were prepared in immunoprecipitation buffer (50 mM Hepes, pH 7.5, 150 mM NaCl, 1 mM EGTA, 0.1% Triton X-100) containing a protease inhibitor cocktail (Roche, 11836153001). Green fluorescent protein-DLK was immunopurified using anti-GFP antibody with Dynabeads Protein G (ThermoFisher

Scientific, 10007D). The substrate GST-MKK4 was purified following a previously described protocol (1). Complexes were incubated for 30 min at 30 °C in 30 μl of kinase buffer (25 mM Hepes, pH 7.2, 10% glycerol, 100 mM NaCl, 20 mM $MgCl_2$, 0.1 mM sodium vanadate, and protease inhibitors) containing 25 μM ATP and 2 μg of GST or GST-MKK4. The reactions were terminated by the addition of Laemmli buffer, boiled, resolved using SDS-PAGE, and subjected to Western blot analysis with an anti-phospho-MKK4 antibody.

Immunohistochemistry

Dorsal root ganglion and sciatic nerve tissues were fixed in 4% paraformaldehyde for 1 h at room temperature immediately after dissection and then immersed in 30% sucrose. Samples were cryopreserved in OCT medium (Tissue-Tek), cryo-sectioned at a thickness of 10 μm, and immunostained as previously described. Briefly, the samples were blocked in blocking solution (5% normal goat serum and 0.1% Triton X-100 in PBS) for 1 h and incubated with primary antibodies diluted in blocking solution overnight at 4 °C. The samples were then rinsed four times with 0.1% Triton X-100 in PBS (PBS-T), incubated with secondary antibodies for 1 h at room temperature, rinsed four times with PBS-T, and mounted using VectaShield (Vector Laboratories, H1000 or H1200). The samples were imaged as z-stacks under a Zeiss LSM800 microscope and z-projected.

In vivo *degeneration assays*

For *in vivo* degeneration assay, the distal part of the sciatic nerve was dissected at 6 mm away from the injury site 3 days after axotomy in control and FKBP8-overexpressing mice in two replicates. Cryopreserved sciatic nerves were cross-sectioned at a thickness of 10 μm, and three sections immunostained with an anti-TUJI antibody were imaged using a Zeiss LSM800 microscope. The images were divided into 100-μm square units. Eight units were randomly selected, and axons with a diameter of more than 5 μm were counted per unit area. We quantified the unfragmented axons in the distal nerve and compared these between FKBP8-overexpressing nerves and controls.

To quantify RGC survival, longitudinal sections of mouse retinas were immunostained for BRN3A. Five sections from two biological replicates were imaged with a Zeiss LSM800 microscope. We quantified BRN3A-positive RGCs in 160 μm unit area and compared between FKBP8-overexpressing retinas and the control.

Optic nerve injury and retina tissue preparation

To expose the optic nerve, the conjunctiva from the orbital region of the eye was cleared, and the optic nerve was crushed for 3 s using a Dumont #5 forceps (Fine Science Tools, 11254-20), taking special care not to damage the sinus vein. Saline solution was applied before and after the ONC injury to protect the eye from desiccation. Three days after injury, the mouse eyes were dissected and fixed *via* immersion in a 4% paraformaldehyde solution for 2 h. After being washed three times in PBS, the eyes were transferred to 30% sucrose solution for 24 h at 4 °C. The optic nerves were dissected out with micro-scissors (Fine Science Tools, 15070-08), the retinas were sectioned at 15 μm in a cryostat, immunostained for BRN3A, and mounted using VectaShield mounting medium (Vector Laboratories, H1000 or H1200).

Data availability

All data is available in the main text.

Acknowledgments—This work was supported by a Korea University grant.

Author contributions—B. L., A. D., V. C., J. E. S., and Y. C. conceptualization; B. L., Y .O., E. C., J. E. S., H. W. C., and Y. C. methodology; B. L., Y. O., E. C., J. E. S., H. W. C., and Y. C. formal analysis; B. L., Y. O., E. C., J. E. S., H. W. C., and Y. C. investigation; J. E. S. and Y. C. resources; J. E. S. and Y. C. funding acquisition; A. D., V. C., J. E. S., and Y. C. supervision; A. D., V. C., J. E. S., and Y. C. project administration; B. L., H. W. C., and Y. C. data curation; B. L., H. W. C., and Y. C. visualization; B. L. and Y. C. writing–original draft; B. L., A. D., V. C., J. E. S., H. W. C., and Y. C. writing–review and editing.

Funding and additional information—This work was supported by a National Research Foundation of Korea (NRF) grant funded by the Korean government (MSIT) (NRF-2019R1A2C1005380 to Y. C., 2016R1A5A2007009 and 2020R1C1C1011074 to J. E. S.).

Conflict of interest—The authors declare that they have no conflicts of interest with the contents of this article.

Abbreviations:—The abbreviations used are: AAV, adeno-associated virus; DLK, dual leucine zipper kinase; DRG, dorsal root ganglion; JNK, c-Jun N-terminal kinase; MKK4, mitogen-activated protein kinase kinase 4; PPI, peptidyl-prolyl isomerase; RGC, retinal ganglion cell; SDS-PAGE, sodium dodecyl sulfate-polyacrylamide gel electrophoresis; SUMO, small ubiquitin-like modifier.

References

1. Holland, S. M., Collura, K. M., Ketschek, A., Noma, K., Ferguson, T. A., Jin, Y., Gallo, G., and Thomas, G. M. (2016) Palmitoylation controls DLK localization, interactions and activity to ensure effective axonal injury signaling. *Proc. Natl. Acad. Sci. U. S. A.* **113**, 763–768
2. Welsbie, D. S., Schirok, H., Mitchell, K., Koch, M., Kim, B.-J., Lobell, M., Patel, A. K., Holton, S., Hristodorov, D., Esteve-Rudd, J., Berlinicke, C., Terjung, C., Hansen, B. S., Werbeck, N., Schubert, W., *et al.* (2018) Identification of a retinal neuroprotective kinase inhibitor with preferential activity against DLK compared to LZK. *Invest. Ophthalmol. Vis. Sci.* **59**, 2493
3. Shin, J. E., Ha, H., Kim, Y. K., Cho, Y., and DiAntonio, A. (2019) DLK regulates a distinctive transcriptional regeneration program after peripheral nerve injury. *Neurobiol. Dis.* **127**, 178–192
4. Shin, J. E., Cho, Y., Beirowski, B., Milbrandt, J., Cavalli, V., and DiAntonio, A. (2012) Dual leucine zipper kinase is required for retrograde injury signaling and axonal regeneration. *Neuron* **74**, 1015–1022
5. Miller, B. R., Press, C., Daniels, R. W., Sasaki, Y., Milbrandt, J., and Diantonio, A. (2009) A dual leucine kinase-dependent axon self-destruction program promotes Wallerian degeneration. *Nat. Neurosci.* **12**, 387–389
6. Nakata, K., Abrams, B., Grill, B., Goncharov, A., Huang, X., Chisholm, A. D., and Jin, Y. (2005) Regulation of a DLK-1 and p38 MAP kinase pathway

by the ubiquitin ligase RPM-1 is required for presynaptic development. *Cell* **120**, 407–420
7. Collins, C. A., Wairkar, Y. P., Johnson, S. L., and DiAntonio, A. (2006) Highwire restrains synaptic growth by attenuating a MAP kinase signal. *Neuron* **51**, 57–69
8. Huntwork-Rodriguez, S., Wang, B., Watkins, T., Ghosh, A. S., Pozniak, C. D., Bustos, D., Newton, K., Kirkpatrick, D. S., and Lewcock, J. W. (2013) JNK-mediated phosphorylation of DLK suppresses its ubiquitination to promote neuronal apoptosis. *J. Cell Biol.* **202**, 747–763
9. Watkins, T. A., Wang, B., Huntwork-Rodriguez, S., Yang, J., Jiang, Z., Eastham-Anderson, J., Modrusan, Z., Kaminker, J. S., Tessier-Lavigne, M., and Lewcock, J. W. (2013) DLK initiates a transcriptional program that couples apoptotic and regenerative responses to axonal injury. *Proc. Natl. Acad. Sci. U. S. A.* **110**, 4039–4044
10. Larhammar, M., Huntwork-Rodriguez, S., Jiang, Z., Solanoy, H., Ghosh, A. S., Wang, B., Kaminker, J. S., Huang, K., Eastham-Anderson, J., Siu, M., Modrusan, Z., Farley, M. M., Tessier-Lavigne, M., Lewcock, J. W., and Watkins, T. A. (2017) Dual leucine zipper kinase-dependent PERK activation contributes to neuronal degeneration following insult. *Elife* **6**, e20725
11. Montersino, A., and Thomas, G. M. (2015) Slippery signaling: Palmitoylation-dependent control of neuronal kinase localization and activity. *Mol. Membr. Biol.* **32**, 179–188
12. Niu, J., Sanders, S. S., Jeong, H. K., Holland, S. M., Sun, Y., Collura, K. M., Hernandez, L. M., Huang, H., Hayden, M. R., Smith, G. M., Hu, Y., Jin, Y., and Thomas, G. M. (2020) Coupled control of distal axon integrity and somal responses to axonal damage by the palmitoyl acyltransferase ZDHHC17. *Cell Rep.* **33**, 108365
13. Martin, D. D. O., Kanuparthi, P. S., Holland, S. M., Sanders, S. S., Jeong, H. K., Einarson, M. B., Jacobson, M. A., and Thomas, G. M. (2019) Identification of novel inhibitors of DLK palmitoylation and signaling by high content screening. *Sci. Rep.* **9**, 1–12
14. Babetto, E., Beirowski, B., Russler, E. V., Milbrandt, J., and DiAntonio, A. (2013) The Phr1 ubiquitin ligase promotes injury-induced axon self-destruction. *Cell Rep.* **3**, 1422–1429
15. Yoo, S.-M., Yamashita, S., Kim, H., Na, D., Lee, H., Kim, S. J., Cho, D.-H., Kanki, T., and Jung, Y.-K. (2020) FKBP8 LIRL-dependent mitochondrial fragmentation facilitates mitophagy under stress conditions. *FASEB J.* **34**, 2944–2957
16. Misaka, T., Murakawa, T., Nishida, K., Omori, Y., Taneike, M., Omiya, S., Molenaar, C., Uno, Y., Yamaguchi, O., Takeda, J., Shah, A. M., and Otsu, K. (2018) FKBP8 protects the heart from hemodynamic stress by preventing the accumulation of misfolded proteins and endoplasmic reticulum-associated apoptosis in mice. *J. Mol. Cell. Cardiol.* **114**, 93–104
17. Lim, G. G., and Lim, K.-L. (2017) Parkin-independent mitophagy-FKBP8 takes the stage. *EMBO Rep.* **18**, 864–865
18. Bhujabal, Z., Birgisdottir, Å. B., Sjøttem, E., Brenne, H. B., Øvervatn, A., Habisov, S., Kirkin, V., Lamark, T., and Johansen, T. (2017) FKBP8 recruits LC3A to mediate Parkin-independent mitophagy. *EMBO Rep.* **18**, 947–961
19. Siekierka, J. J., Hung, S. H., Poe, M., Lin, C. S., and Sigal, N. H. (1989) A cytosolic binding protein for the immunosuppressant FK506 has peptidyl-prolyl isomerase activity but is distinct from cyclophilin. *Nature* **341**, 755–757
20. Heitman, J., Movva, N. R., and Hall, M. N. (1992) Proline isomerases at the crossroads of protein folding, signal transduction, and immunosuppression. *New Biol.* **4**, 448–460
21. Schmid, F. X., Mayr, L. M., Mücke, M., and Schönbrunner, E. R. (1993) Prolyl isomerases: Role in protein folding. *Adv. Protein Chem.* **44**, 25–66
22. Kang, C. B., Hong, Y., Dhe-Paganon, S., and Yoon, H. S. (2008) FKBP family proteins: Immunophilins with versatile biological functions. *Neurosignals* **16**, 318–325
23. Ghartey-Kwansah, G., Li, Z., Feng, R., Wang, L., Zhou, X., Chen, F. Z., Xu, M. M., Jones, O., Mu, Y., Chen, S., Bryant, J., Isaacs, W. B., Ma, J., and Xu, X. (2018) Comparative analysis of FKBP family protein: Evaluation, structure, and function in mammals and Drosophila melanogaster. *BMC Dev. Biol.* **18**, 7
24. Tong, M., and Jiang, Y. (2015) FK506-binding proteins and their diverse functions. *Curr. Mol. Pharmacol.* **9**, 48–65
25. Shin, J. E., Ha, H., Cho, E. H., Kim, Y. K., and Cho, Y. (2018) Comparative analysis of the transcriptome of injured nerve segments reveals spatiotemporal responses to neural damage in mice. *J. Comp. Neurol.* **526**, 1195–1208
26. [preprint] Lee, B., Lee, J., Jeon, Y., Kim, H., Kwon, M., Shin, J. E., and Cho, Y. (2021) Promoting axon regeneration by enhancing the non-coding function of the injury-responsive coding gene Gpr151. *bioRxiv*. https://doi.org/10.1101/2021.02.19.431965
27. Cho, Y., Sloutsky, R., Naegle, K. M., and Cavalli, V. (2013) Injury-induced HDAC5 nuclear export is essential for axon regeneration. *Cell* **155**, 894–908
28. Tedeschi, A., and Bradke, F. (2013) The DLK signalling pathway - a double-edged sword in neural development and regeneration. *EMBO Rep.* **14**, 605–614
29. Fernandes, K. A., Harder, J. M., John, S. W., Shrager, P., and Libby, R. T. (2014) DLK-dependent signaling is important for somal but not axonal degeneration of retinal ganglion cells following axonal injury. *Neurobiol. Dis.* **69**, 108–116
30. Summers, D. W., Frey, E., Walker, L. J., Milbrandt, J., and DiAntonio, A. (2020) DLK activation synergizes with mitochondrial dysfunction to downregulate axon survival factors and promote SARM1-dependent axon degeneration. *Mol. Neurobiol.* **57**, 1146–1158
31. Valakh, V., Frey, E., Babetto, E., Walker, L. J., and DiAntonio, A. (2015) Cytoskeletal disruption activates the DLK/JNK pathway, which promotes axonal regeneration and mimics a preconditioning injury. *Neurobiol. Dis.* **77**, 13–25
32. Jin, Y., and Zheng, B. (2019) Multitasking: Dual leucine zipper-bearing kinases in neuronal development and stress management. *Annu. Rev. Cell Dev. Biol.* **35**, 501–521
33. Geden, M. J., and Deshmukh, M. (2016) Axon degeneration: Context defines distinct pathways. *Curr. Opin. Neurobiol.* **39**, 108–115
34. DiAntonio, A. (2019) Axon degeneration: Mechanistic insights lead to therapeutic opportunities for the prevention and treatment of peripheral neuropathy. *Pain* **160**, S17–S22
35. Cho, Y., Di Liberto, V., Carlin, D., Abe, N., Li, K. H., Burlingame, A. L., Guan, S., Michaelevski, I., and Cavalli, V. (2014) Syntaxin13 expression is regulated by mammalian target of rapamycin (mTOR) in injured neurons to promote axon regeneration. *J. Biol. Chem.* **289**, 15820–15832
36. Lee, J., Shin, J. E., Lee, B., Kim, H., Jeon, Y., Ahn, S. H., Chi, S. W., and Cho, Y. (2020) The stem cell marker Prom1 promotes axon regeneration by down-regulating cholesterol synthesis via Smad signaling. *Proc. Natl. Acad. Sci. U. S. A.* **117**, 15955–15966
37. Cho, Y., and Cavalli, V. (2012) HDAC5 is a novel injury-regulated tubulin deacetylase controlling axon regeneration. *EMBO J.* **31**, 3063–3078
38. Jeon, Y., Shin, J. E., Kwon, M., Cho, E., Cavalli, V., and Cho, Y. (2021) In vivo gene delivery of STC2 promotes axon regeneration in sciatic nerves. *Mol. Neurobiol.* **58**, 750–760